

Systematic variation of fission barrier heights for symmetric and asymmetric mass divisions

T. Ohtsuki

Laboratory of Nuclear Science, Faculty of Science, Tohoku University, Mikamine, Taihaku, Sendai, 982 Japan

H. Nakahara

Department of Chemistry, Faculty of Science, Tokyo Metropolitan University, Minami-Ohsawa, Hachioji, Tokyo, 192-03 Japan

Y. Nagame

Japan Atomic Energy Research Institute (JAERI), Tokai, Ibaraki, 319-11 Japan

(Received 2 April 1993)

The excitation functions and the mass yield curves for proton-induced fissions of ^{233}U , ^{235}U , ^{236}U , ^{237}Np , ^{239}Pu , ^{242}Pu , ^{244}Pu , ^{241}Am , and ^{243}Am targets were studied. The excitation functions for near-symmetrically divided fragments were found quite different in shapes and threshold energies from those of asymmetrically divided ones in all the fissioning systems studied. In order to obtain the fission barrier heights for symmetric and asymmetric mass division, the conventional Bohr-Wheeler type calculations for the competition between fission and neutron emission were performed. In the calculation, two independent fission channels, symmetric and asymmetric, were assumed, and fission barrier heights and level density parameters that could best reproduce the shapes of the excitation functions (incident energy dependence) of typical symmetric and asymmetric products were deduced. Barrier heights for symmetric and asymmetric mass divisions both decrease as the mass of fissioning nuclide A_f increases, and they also exhibit slight dependence on the atomic number. Difference between the two barrier heights is 2.0–2.5 MeV in the region of $A_f = 236$ –245. From similar analysis of excitation function data reported in literature, it is found that the difference changes from a large positive value for $N \sim 150$, neutron number of the fissioning nuclide, to a large negative value for $N \sim 126$, and the two barrier heights become comparable at $N = 135$ –138.

PACS number(s): 25.85.Ge, 27.90.+b

I. INTRODUCTION

Many experimental data on mass and kinetic-energy distributions have suggested the fact that the shell structure of the two final fragments plays an important role in deciding the mass division. It is also reasonable to think from the studies on the intermediate structure in the fission cross sections that the fission probability is determined by the state density around the fission barrier. The question is, then, is there any experimental evidence that supports the influence of the nuclear structure near the barrier on the final mass division? It has long been known that the yields of symmetrically and asymmetrically divided products vary differently with the incident energy, possibly due to different threshold energies. These observations have led Turkevich and Niday [1] to suggest, as an operational principle, that the fission has “two independent modes,” one associated with symmetric and the other with the asymmetric mass distributions. The two-mode character was also supported by Britt, Wegner, and Gursky [2] who measured the kinetic-energy distribution of fission fragments as a function of mass ratio. Konecny, Specht, and Weber [3] and Weber *et al.* [4] carefully measured fission probabilities and fragment anisotropies of $^{226-228}\text{Ac}$, $^{225,227}\text{Ra}$, and ^{228}Ra by direct reactions and found different thresholds for symmetric and asymmetric fission and different angular anisotropies for the two components at the energy

close to the fission barrier.

On the theoretical side, the importance of the saddle point in deciding the final mass division was claimed by the charged-liquid-drop model according to which there was no quasistable state after the descent from the saddle toward scission, the dynamical motion determining the fate of mass division [5]. Although the liquid-drop model could only give a saddle with reflection symmetry which resulted in the symmetric mass division, Möller and Nilsson [6] first pointed out with incorporation of the shell effect by the Strutinsky prescription [7,8] that a reflection asymmetric saddle was energetically more favored to the symmetric one at the outer barrier. It was shown that there could be some correlation between the calculated saddle mass asymmetry and the experimentally observed mean asymmetry [9–11].

To advance these experimental and theoretical studies, systematic studies on excitation energy dependence of mass yield curves are further needed from the light to the heavy actinide region. Such investigations had been carried out for the proton-induced fission of ^{232}Th , ^{233}U , ^{235}U , ^{236}U , ^{237}Np , ^{239}Pu , ^{242}Pu , ^{244}Pu , ^{241}Am , and ^{243}Am by the present authors [12,13]. The aim of the present paper is to study how, in terms of the “two-mode” process, the two kinds of fission barrier heights vary as a function of the number of protons and neutrons of the fissioning compound nucleus. For this purpose, the excitation functions of fission fragments reported were ana-

lyzed by the Bohr-Wheeler-type statistical calculation of fission and evaporation.

II. STATISTICAL MODEL CALCULATION

A. Systematical trend of experimental data

Mass yield curves of proton induced fission for ^{233}U , ^{235}U , ^{236}U , ^{237}Np , ^{239}Pu , ^{242}Pu , ^{244}Pu , ^{241}Am , and ^{243}Am were obtained from the observed cross section (mb) of each fission product and have been reported in a separate

paper [12] together with the experimental procedure and data treatment. The range of proton energies considered in the present work is listed in Table I for each target nucleus. The mass divisions were mainly asymmetric and the probability of symmetric fission increased more rapidly as a function of the excitation energy compared with that of asymmetric fission in all reactions.

The typical excitation functions of asymmetrically divided fission products are different from those of symmetrically divided ones as shown in Figs. 1(a)–1(g). The relative yield of the symmetric to the asymmetric fission is

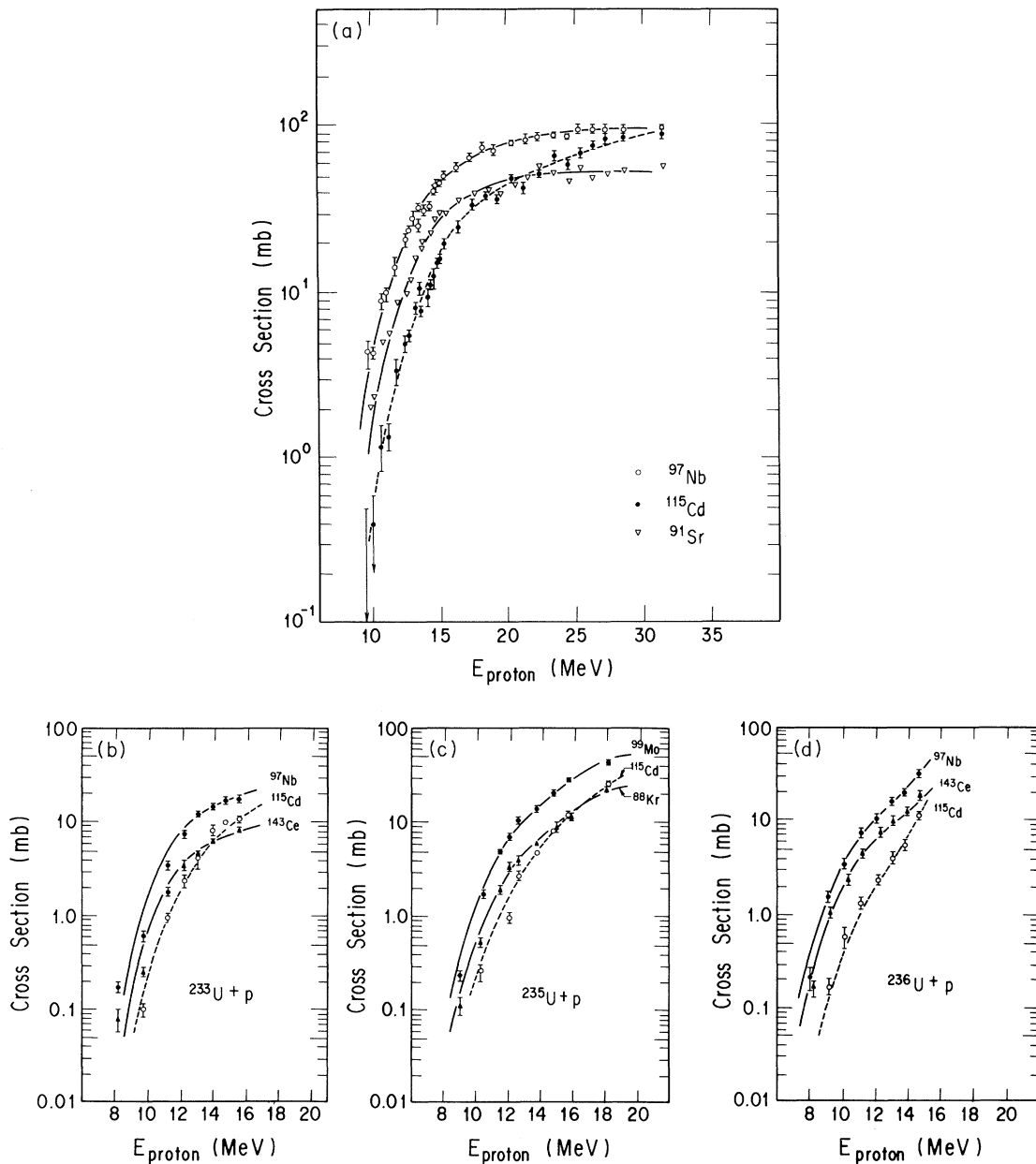


FIG. 1. (a) Comparison of the calculated excitation functions with the observed data for $^{237}\text{Np} + p$. Solid line indicates the excitation function for asymmetric mass division, and the dashed line indicates the excitation function for symmetric one reproduced by means of statistical calculation. (b)–(g) Same as (a) for $^{233}\text{U} + p$, $^{235}\text{U} + p$, $^{236}\text{U} + p$, $^{239}\text{Pu} + p$, $^{244}\text{Pu} + p$, and $^{241}\text{Am} + p$.

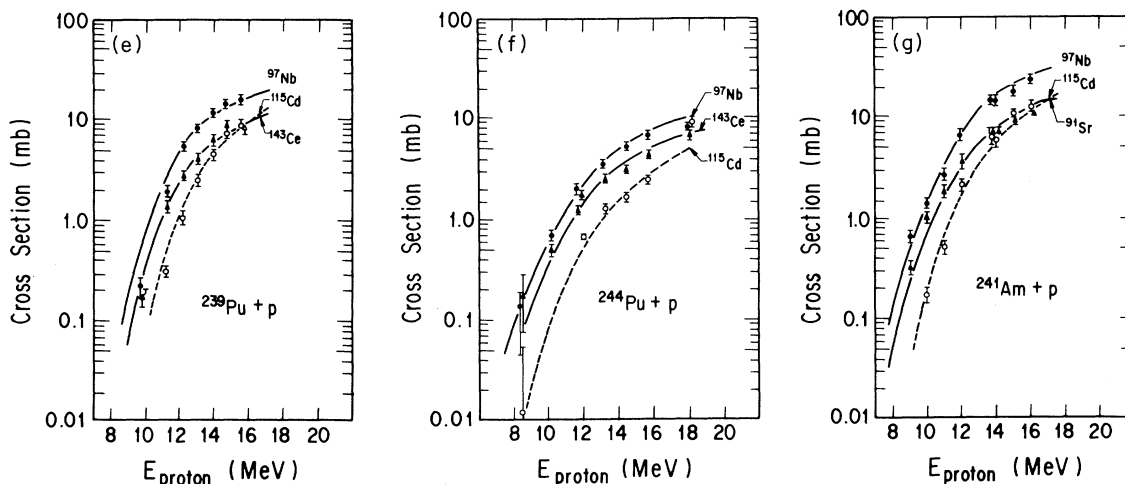


FIG. 1. (Continued).

represented by the peak-to-valley ratio of the mass yield curve as a function of excitation energy and shown in Figs. 2(a) and 2(b). For more detail investigation, incident energy dependence of the cross section for each fragment mass (A) to ^{97}Nb , $\sigma(A)/\sigma(^{97}\text{Nb})$, is investigated. The ratios of the $\sigma(A)/\sigma(^{97}\text{Nb})$ for $^{237}\text{Np}+p$ are plotted in Fig. 3 as a function of the incident energy of protons. As can be seen from the figure, the value of the $\sigma(A)/\sigma(^{97}\text{Nb})$ for symmetric regions (such as ^{115}Cd) increases from a small value toward unity with an increase of the proton energy, i.e., the probability of symmetric fission increases more rapidly compared with that of asymmetric fission in all reaction systems. However, the cross-section ratios for the asymmetric products ($A < 105$ and $131 < A$) are rather independent of proton energy. Thus, they can be grouped into two as a first approximation, and within each group the yield ratio among any two products shows no incident energy dependence except for some minor fluctuations. (It is to be noted that the yield ratios are somewhat different in the region intermediate between the symmetric and asymmetric, but they may be interpreted as a mixture of the asymmetric and symmetric groups.)

These systematic studies of incident energy dependence strongly suggests the existence of at least two different threshold energies, one for symmetric mass division and the other for asymmetric one for fission of actinides ranging from $Z = 91$ through 96.

B. General consideration

The two kinds of threshold energies in the process of deformation leading to mass division may be interpreted in two ways. The first postulate is that there are two different saddles which determine the fission rates of symmetric and asymmetric mass division independently although some fluctuation of mass division will be introduced during the descent from the saddle to scission. This postulate was first introduced by Turkevich and Niday [1] in 1951, and called "two-mode" hypothesis.

Theoretically, Pashkevich [16] and Brosa and co-workers [17,18] claim that there are two kinds of saddles in the potential energy surface, one symmetric and the other asymmetric with respect to the reflection plane perpendicular to the nuclear symmetry axis. The second postulate is that there is only one-saddle at the deformation of the second barrier which is reflection asymmetric in shape [6] according to the microscopic-macroscopic calculation using the Strutinsky prescription [7,8] and this saddle determines the fission rate. The threshold for symmetric mass division is considered to originate from a static or dynamical barrier during the motion from the saddle toward scission, thus the process requiring extra energy at the saddle point for symmetric division. Möller, Nix, and Swiatecki [19] recently claims that there is such a static barrier in the potential energy surface of ^{258}Fm but no such barriers for lighter actinide nuclides.

According to the second postulate, the energy dependence of the yields $\sigma(A, E)$ of typical symmetric and asymmetric fission products may be described by

TABLE I. Reactions of proton-induced fissions and the range of the incident energy.

Reaction	E_{proton} (MeV)
$^{232}\text{Th}+p^a$	9–22
$^{233}\text{U}+p$	8–16
$^{235}\text{U}+p$	9–18
$^{236}\text{U}+p$	9–16
$^{238}\text{U}+p^b$	10–25
$^{237}\text{Np}+p$	10–32
$^{239}\text{Pu}+p$	10–18
$^{242}\text{Pu}+p$	12, 18
$^{244}\text{Pu}+p$	10–18
$^{241}\text{Am}+p$	9–16
$^{243}\text{Am}+p$	10–16

^aFrom Ref. [14].^bFrom Ref. [15].

$$\frac{\sigma_s(A,E)}{\sigma_R(E)} = \Gamma_f(E,E_f)P(E,E_f+\delta) \frac{y_s(A)}{\Gamma_t(E)}, \quad (1)$$

$$\frac{\sigma_a(A,E)}{\sigma_R(E)} = \Gamma_f(E,E_f)[1-P(E,E_f+\delta)] \frac{y_a(A)}{\Gamma_t(E)}, \quad (2)$$

where $\Gamma_f(E,E_f)$ is the total fission width in the decay of

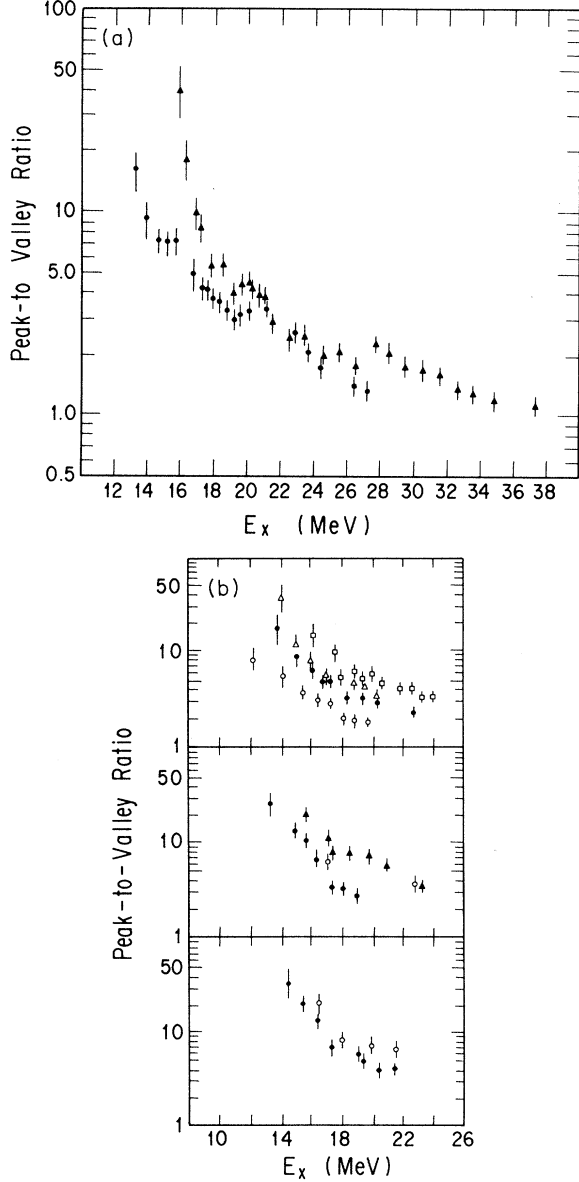


FIG. 2. (a) Variation of the peak-to-valley ratio for $^{237}\text{Np}+p$ (closed triangles) and $^{232}\text{Th}+p$ (closed circles) from Ref. [14]. (b) Variation of the peak-to-valley ratio for various targets as a function of the excitation energy. Upper part shows $Z=93$ (open squares indicate ratio for $^{238}\text{U}+p$, open triangles for $^{236}\text{U}+p$, closed circles for $^{235}\text{U}+p$, and open circles for $^{233}\text{U}+p$), middle part for $Z=95$ (solid triangles for $^{244}\text{Pu}+p$, open circles for $^{242}\text{Pu}+p$, and closed circles for $^{239}\text{Pu}+p$), and bottom part for $Z=96$ (open circles for $^{243}\text{Am}+p$ and closed circles for $^{241}\text{Am}+p$).

the compound nucleus with E and E_f being the excitation energy and the barrier height of the saddle. $\Gamma_t(E)$ and $\sigma_R(E)$ are the total decay width and the formation cross section of the compound nucleus, respectively. $P(E,E_f+\delta)$ is a fraction of the fission width leading to symmetric mass division and it depends on the extra energy δ required for going toward mass symmetric deformation from the saddle configuration. $y(A)$ is a fraction of either symmetric or asymmetric fission resulting in the final fragment mass A . The function $y(A)$ is independent of E since the yield ratios among symmetric products themselves and asymmetric ones themselves are independent of the incident proton energy to the first approximation within the energy range studied as shown in Fig. 3 and discussed above.

At present, experimental data are analyzed with an assumption of two fission modes and their threshold energies are derived. Although the two-mode hypothesis is conceptually different from the model described by Eqs. (1) and (2), they are identical in appearance for deriving threshold energies. Let the fission width decaying through the symmetric and asymmetric saddle be $\Gamma_{f,s}(E,E_{f,s})$ and $\Gamma_{f,a}(E,E_{f,a})$, respectively. Then, the yields of typical symmetric and asymmetric fission products can be described by

$$\frac{\sigma_s(A,E)}{\sigma_R(E)} = \Gamma_{f,s}(E,E_{f,s}) \frac{y_s(A)}{\Gamma_t(E)}, \quad (3)$$

$$\frac{\sigma_a(A,E)}{\sigma_R(E)} = \Gamma_{f,a}(E,E_{f,a}) \frac{y_a(A)}{\Gamma_t(E)}, \quad (4)$$

where $E_{f,s}$ and $E_{f,a}$ are the barrier height of the symmetric and asymmetric saddle, respectively. From comparison of Eqs. (1) and (3), and (2) with (4)

$$\Gamma_{f,s}(E,E_{f,s}) \propto \Gamma_f(E,E_f)P(E,E_f+\delta), \quad (5)$$

$$\Gamma_{f,a}(E,E_{f,a}) \propto \Gamma_f(E,E_f)[1-P(E,E_f+\delta)]. \quad (6)$$

Therefore, even though the two-mode hypothesis is used in the following analysis and $E_{f,s}$ and $E_{f,a}$ are derived, the $E_{f,s}$ corresponds to $(E_f+\delta)$ and $(E_{f,s}-E_{f,a})=\delta$, the extra energy discussed in the second postulate of the discussion above so long as the probability $P(E,E_f+\delta)$ follows the statistical argument.

C. Statistical model calculation

We can calculate the competition of fission to neutron emission Γ_f/Γ_n , where Γ_n is the neutron emission width, with the Bohr-Wheeler-type [20] statistical calculation. If the existence of two different saddles, symmetric and asymmetric, is assumed as in the two-mode hypothesis, the competition between the symmetric fission mode and the asymmetric one should be included in the calculation as separate exit channels:

$$\Gamma_t = \Gamma_n + \Gamma_{f,s} + \Gamma_{f,a} + \Gamma_\gamma, \quad (7)$$

$$\Gamma_f = \Gamma_{f,s} + \Gamma_{f,a}. \quad (8)$$

There are many parameters involved in the calculation,

but they can be determined rather unambiguously by choosing a set of parameters that gives the best fit to the experimental data such as $\sigma_f(E)$, $\sigma_s(A,E)$, $\sigma_a(A,E)$, and peak-to-valley ratios observed in this work. [Although total symmetric and asymmetric fission cross sec-

tions, $\Gamma_{f,s}(E,E_{f,s})$ and $\Gamma_{f,a}(E,E_{f,a})$, have not been observed, the energy dependence of $\Gamma_f(E,E_f)$ should be the same with that of $\sigma(A,E)$ as $y(A)$ is independent of E in Eqs. (3) and (4).] $\Gamma_{f,s}$ and $\Gamma_{f,a}$ can be expressed with the level density and the barrier penetration formula as

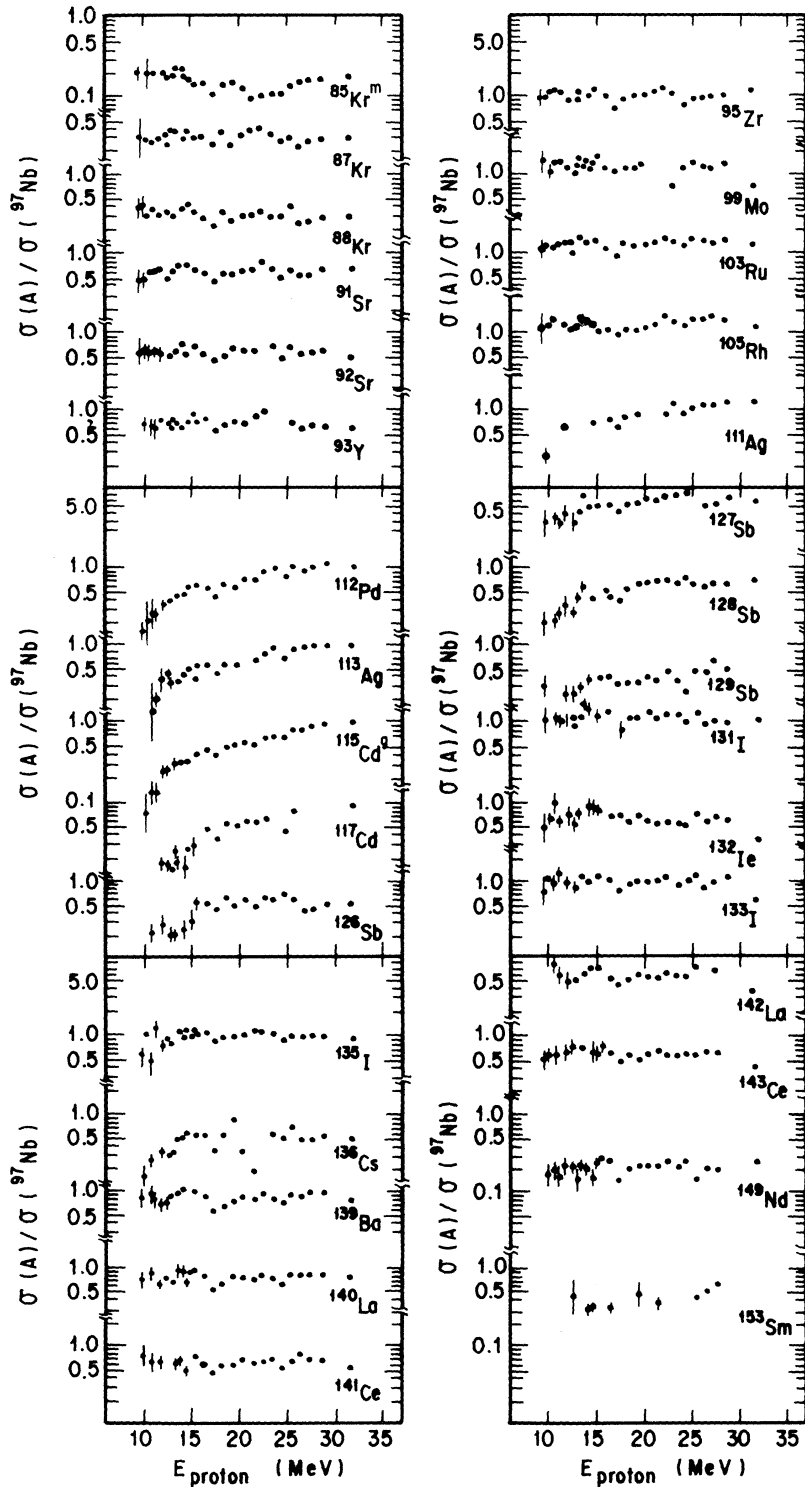


FIG. 3. Cross-section ratios $\sigma(A)/\sigma(^{97}\text{Nb})$ as a function of the incident proton energy for the $^{237}\text{Np}+p$ fission.

$$\Gamma_{f,s} = \frac{D}{2\pi} \int_0^E \left[\frac{\rho(E - E_{f,s} - \kappa)}{1 + \exp(-2\pi\kappa/\hbar\omega_s)} \right] d\kappa, \quad (9)$$

$$\Gamma_{f,a} = \frac{D}{2\pi} \int_0^E \left[\frac{\rho(E - E_{f,a} - \kappa)}{1 + \exp(-2\pi\kappa/\hbar\omega_a)} \right] d\kappa, \quad (10)$$

where D is the average level spacing of the compound nucleus and κ is the kinetic energy in the fission degree of freedom. The parameters involved in the calculation are a_n the level density parameter at ground-state deformation, $a_{f,s}$ and $a_{f,a}$ the level density parameter at symmetric and asymmetric saddle-point deformation, respectively, $\hbar\omega_s$, and $\hbar\omega_a$ the barrier curvature energy for symmetric and asymmetric fission, respectively, $E_{f,s1}$, $E_{f,s2}$, $E_{f,s3}$, and $E_{f,s4}$ the symmetric fission barrier height for first, second, third, and fourth chance fission, respectively, and $E_{f,a1}$, $E_{f,a2}$, $E_{f,a3}$, and $E_{f,a4}$ the asymmetric fission barrier height for first, second, third, and fourth chance fission, respectively. The calculation was performed by means of the ALICE code [21] which was modified to include the symmetric fission barrier and asymmetric fission barrier as parameters.

In the calculation, fission competition is considered up to the fourth chance fission which is the fission of a nucleus formed after evaporation of three neutrons from the compound nucleus. As for the barrier shape, it would be most appropriate to use a double-humped barrier whose existence is well established by experimental data. Indeed, for detailed study of the double-humped potential surface, fission cross sections should be observed at excitation energies comparable to the barrier heights, and the data have to be analyzed by taking into considerations fission channels of specific spins and parities, transmission coefficient through a double-humped fission barriers, and the coupling between the levels in well I and II [22,23]. But as the energy considered in the present calculation is rather high and a subtle difference in the barrier penetration does not essentially affect the final result, only a single barrier is considered in the calculation in order not to complicate the calculation by introducing many more unknown parameters. (In Ref. [4], the ratios of symmetric to asymmetric fission probabilities were observed as a function of excitation energy and the data were analyzed by use of a double-humped fission barrier.

It was confirmed in the present work that the second barrier heights they derived for symmetric and asymmetric fission, could also as well be deduced by applying the single-barrier analysis to their data observed at excitation energies more than 2 MeV above the barriers.) It is to be noted that most of the fission threshold energies or the fission barrier heights reported in literature are $E_{f,a}$ since the fraction of symmetric fission is small and it does not alter the results obtained by fitting theoretical calculation to the experimental excitation function of total fission cross section.

The calculation was repeated many times by varying the free parameters until a best set of parameters was obtained that could reproduce typical shapes of the excitation functions observed for symmetrically and asymmetrically divided products, and the peak-to-valley ratios. In the fitting procedure, the barrier heights were first varied by setting the level density parameters as $a_{f,a} = a_{f,s} = 1.05$. However, the calculated peak-to-valley ratios were larger than the experimental values even if unrealistic barrier heights were chosen. Therefore, the level density parameters for symmetric fission had to be taken larger than those for the asymmetric $a_{f,s} > a_{f,a}$ by 3–13%, and, then, the barrier heights were changed for the best fit to the observed peak-to-valley ratios and the excitation functions. This choice of level density parameters is qualitatively in agreement with the earlier observation by Gavron *et al.* [24] who pointed out the necessity of including γ deformation for the reflection-symmetric second saddle. The barrier curvature parameters ($\hbar\omega$) were fixed at the commonly used value of 1.0 MeV because they were insensitive to the fitting in the present excitation energy region. The level density parameter a_n for neutron emission was fixed to $A/8$ in accordance with the value deduced from neutron capture data.

D. Result of calculations

The parameters deduced are summarized in Table II. The $a_{f,a}$ were around 1.02–1.07 times larger than a_n , and $a_{f,s}$ around 1.12–1.15 times larger than a_n . The asymmetric fission barrier heights for the first chance fission are compared with reported values [22,23] and tabulated in Table III. The uncertainties of the deduced

TABLE II. Parameters used in the statistical model calculation for first chance fission.

Reaction	$E_{f,a}$ (MeV)	$E_{f,s}$ (MeV)	$a_{f,a}/a_n$	$a_{f,s}/a_n$	$E_{f,s} - E_{f,a}$ (MeV)
$^{232}\text{Th} + p$	5.9	8.8	1.02	1.17	2.9
$^{233}\text{U} + p$	5.8	6.8	1.05	1.22	1.0
$^{235}\text{U} + p$	5.7	7.7	1.05	1.20	2.0
$^{236}\text{U} + p$	6.0	8.1	1.05	1.20	2.1
$^{238}\text{U} + p$	5.3	7.4	1.05	1.21	2.1
$^{237}\text{Np} + p$	5.9	7.9	1.05	1.21	2.0
$^{239}\text{Pu} + p$	5.1	7.2	1.05	1.21	2.1
$^{242}\text{Pu} + p$	5.0	7.0	1.05	1.20	2.0
$^{244}\text{Pu} + p$	4.7	6.8	1.06	1.19	2.1
$^{241}\text{Am} + p$	4.4	7.0	1.07	1.22	2.6
$^{243}\text{Am} + p$	4.3	6.6	1.06	1.17	2.3

TABLE III. Comparison of fission barrier heights deduced in the present work with literature values. E_f indicates the asymmetric barrier height obtained from present work. E_A and E_B for the first and second barrier heights from Refs. [23,22], respectively.

Fissioning Nuclei	$a_{f,a}/a_n$ (This work)	E_f (MeV)	E_A (MeV) (Ref. [23])	E_B (MeV) (Ref. [23])	E_A (MeV) (Ref. [22])	E_B (MeV) (Ref. [22])
^{233}Pa	1.02	5.9	6.2	6.2	5.8	6.0
^{234}Np	1.05	5.8	5.7	5.2	5.3	5.0
^{236}Np	1.05	5.7	5.9	5.7	5.7	5.2
^{237}Np	1.05	6.0	5.9	5.6	5.7	5.5
^{239}Np	1.05	5.3	6.1	5.6	5.8	5.5
^{238}Pu	1.05	5.9	5.5	5.0	5.9	5.2
^{240}Am	1.05	5.1	6.5	5.4	6.3	4.8
^{243}Am	1.05	5.0	6.2	5.6	6.0	4.8
^{245}Am	1.06	4.7	6.2	5.3	5.9	5.8
^{242}Cm	1.07	4.4	5.8	4.0		
^{244}Cm	1.06	4.3	5.8	4.3	6.2	4.2

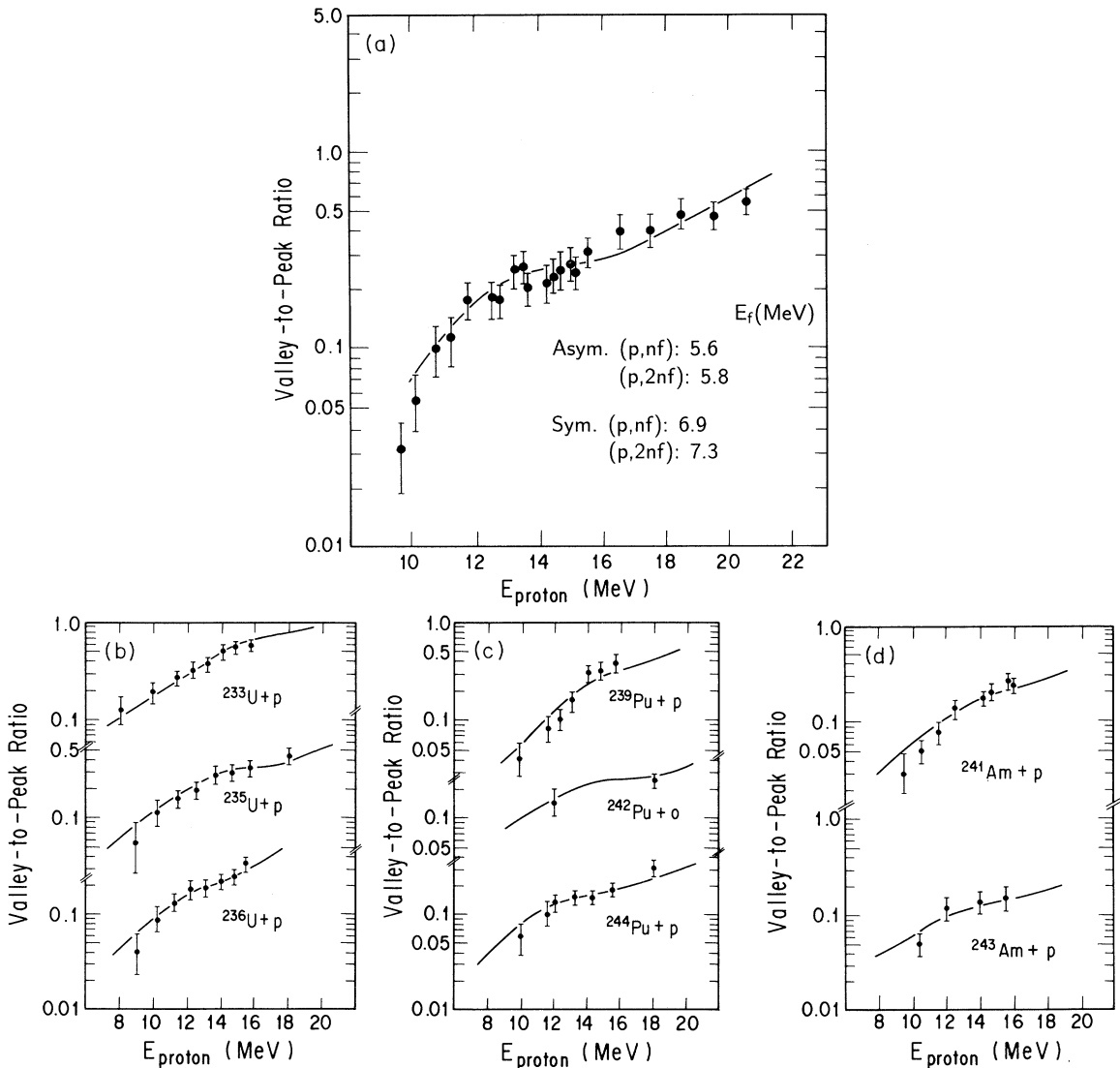


FIG. 4. (a) Symmetric to asymmetric yield ratios as a function of proton energy for $^{237}\text{Np}+p$. Solid line indicate the valley-to-peak ratio reproduced by means of statistical calculation using the parameters shown in Table II. (b)–(d) Same as (a) for $^{233}\text{U}+p$, $^{235}\text{U}+p$, $^{236}\text{U}+p$, $^{239}\text{Pu}+p$, $^{242}\text{Pu}+o$, $^{244}\text{Pu}+p$, $^{241}\text{Am}+p$, and $^{243}\text{Am}+p$. For details of barrier heights of second and third chance fission, see Ref. [29].

barrier heights are estimated to be about ~ 0.3 MeV by considering the ambiguity involved in the fitting procedure. The reproduced shapes of excitation functions for typical symmetric and asymmetric products are shown in Figs. 1(a)–1(g) by solid and dashed curves. Reproduced energy dependence of valley-to-peak ratios are also shown by solid lines in Figs. 4(a)–4(d).

III. DISCUSSIONS

The level density parameters for symmetric and asymmetric saddles deduced in the present analysis are shown in Table II. It should be noted that the level density parameters for the asymmetric fission mode ($a_{f,a}$) stay around 1.02–1.07, though the level density parameters ($a_{f,s}$) for the symmetric fission mode remain constant at around 1.17–1.22. These results are in agreement with those reported by Tang and Wilhelmy [25], and Gavron *et al.* [24].

The evaluated fission barrier heights for the symmetric and asymmetric fission as a function of the mass of the fissioning nucleus are shown in Fig. 5, and they are also plotted against the neutron number in Fig. 6. Triangles indicate symmetric fission barrier heights ($E_{f,s}$), squares are for the asymmetric ones ($E_{f,a}$), and closed circles for the difference between those of the symmetric and the asymmetric fissions ($E_{f,s} - E_{f,a}$). Dashed lines and dot-dashed lines show the results of the theoretical calculation of the asymmetric second barrier and the difference between the symmetric and asymmetric second barrier heights, respectively, for even-even isotopes of U, Pu, and Cm reported by Möller and co-worker [11,26]. As most

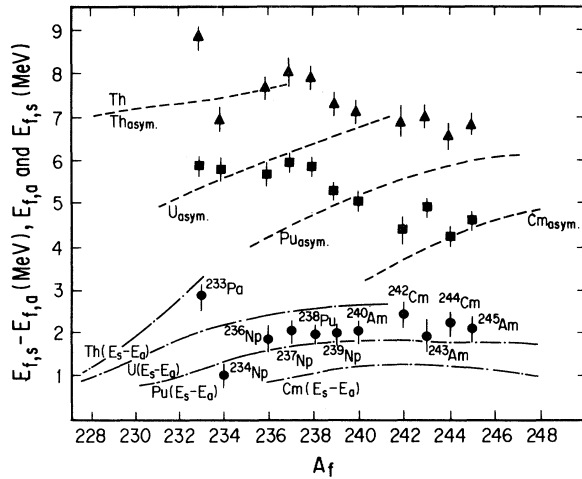


FIG. 5. Deduced fission barrier heights and the difference in the barrier heights between symmetric fission and asymmetric one as a function of the mass number of the fissioning nucleus. Closed triangles indicate symmetric barrier height, closed squares indicate asymmetric one, and closed circles indicate the difference in barrier heights between symmetric fission and asymmetric one. Dashed lines indicate asymmetric second barrier height predicted by Möller and co-worker [11,26], dot-dashed lines for the predicted difference between the symmetric and asymmetric second barrier heights.

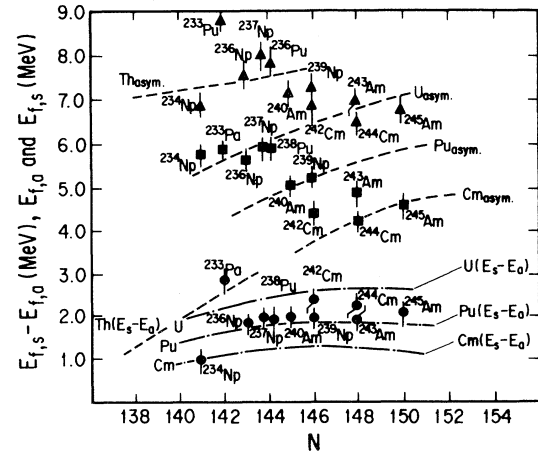


FIG. 6. Same as Fig. 5, but plotted against the neutron number of fissioning nuclide.

of the fissioning nuclides investigated in this study are either even odd, odd even, or odd odd in the proton and neutron numbers, our results cannot be directly compared with their theoretical results, but the latter are shown in the figures for reference. From the figure, it is found that the symmetric fission barrier ($E_{f,s}$) is anomalously high for ^{233}Pa and rather small for ^{234}Np , but it tends to decrease as A_f or N becomes larger.

The difference between the symmetric and the asymmetric fission barrier ($E_{f,s} - E_{f,a}$) is rather constant in this region except for ^{233}Pa and ^{234}Np . Among the fissioning nuclides of Np isotopes, the symmetric and asymmetric barrier heights increase with the neutron number up to $N = 144$ and decrease at $N = 146$. It is to be remembered that the barrier heights in this work were obtained by simply applying the Bohr-Wheeler-type calculation with a single fission barrier along the respective fission path. However, as shown in Table III, the asymmetric barrier heights obtained in this work are closer to the second asymmetric barrier heights rather than to the higher first barrier heights reported by Bjørnholm and Lynn [23] especially for the nuclides with $Z = 95$ and 96 . This result is reasonable since in the present work the statistical analysis was applied to the cross-section data observed at excitation energies larger than 15 MeV. At excitation energies well above the barrier, the effect of barriers on the transmission is small and the excitation energy and level density at the saddle mostly determine the fission decay width.

The difference between the two barriers or the extra energy required for the symmetric mass division over the asymmetric one ($E_{f,s} - E_{f,a}$) as a function of neutron number is shown in Fig. 7 for the wider range of fissioning nuclides from Po to Am. The values of ($E_{f,s} - E_{f,a}$) reported by Specht [27] and Weber *et al.* [4] for the Ra and Ac region and by Itkis *et al.* [28] for the Po and At region are also shown in the figure for lighter fission systems. The ($E_{f,s} - E_{f,a}$) value changes from a large positive value at $N \sim 150$ to a large negative value at $N \sim 126$, and the two barrier heights become comparable at

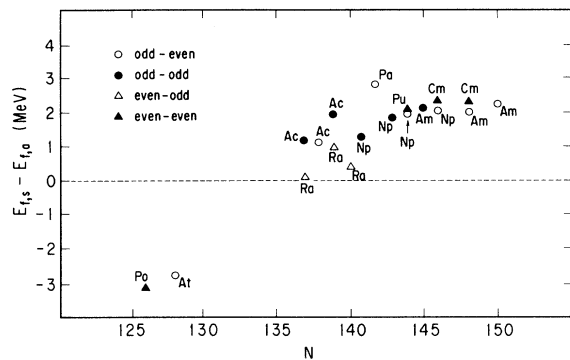


FIG. 7. Difference in the barrier heights ($E_{f,s} - E_{f,a}$) in MeV, as a function of the neutron number of either compound nucleus or fissioning nucleus. The values for Ra and Ac isotopes are from Refs. [4,27], and those for Po and At isotopes are from Ref. [28].

$N = 135-138$. This trend indicates that the shape of the mass distribution systematically changes from symmetric for the Bi and Po region, triple humped for the Ra and Ac region, and to double humped for most of actinides.

In Fig. 8 are plotted the location in the Z - N plane of the fissioning nuclides for which symmetric and asymmetric fission thresholds have been deduced semiempirically. The broken line shows the theoretically predicted dividing line where the symmetric and asymmetric second barrier heights become equal according to the microscopic-macroscopic calculation of the potential energy surface by Möller and co-worker [11,26]. Further investigation is required to define the area in the (Z, N) plane where the $(E_{f,s} - E_{f,a})$ value becomes equal and to seek the correlation between the mass division mechanism and the nuclear shell structure of the fissioning nuclide.

IV. CONCLUSION

For the interpretation of the observed excitation functions of fission products in proton induced fission of ^{233}U , ^{235}U , ^{236}U , ^{237}Np , ^{239}Pu , ^{242}Pu , ^{244}Pu , ^{241}Am , and ^{243}Am targets, statistical model calculations were performed by including the competition of the symmetric fission process and asymmetric one with neutron emission. With this statistical calculation, shape of the excitation functions and the peak-to-valley ratios could well be reproduced using reasonable parameters. It is found that the

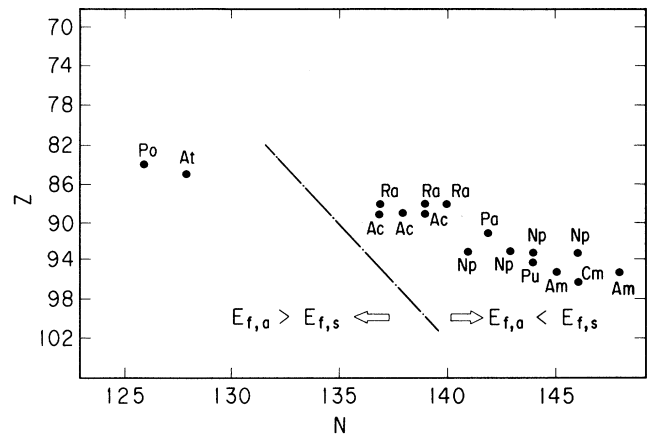


FIG. 8. Z and N plot showing the fissioning nucleus for which symmetric and asymmetric fission threshold energies have been determined empirically. The broken line shows the demarcation where the heights of the symmetric and asymmetric second barriers become equal according to the prediction by microscopic-macroscopic calculation of the potential energy surface [11,26].

fission barrier heights obtained for asymmetric and symmetric mass divisions decrease as the mass of the fissioning nucleus increases. The difference between the two barrier heights ($E_s - E_a$) was found to change from a large positive value for $N \sim 150$ to a large negative value for $N \sim 126$, and the two become comparable at $N = 135-138$. This trend is in agreement with the previously known fact that the shape of the mass distribution changes from symmetric mass distribution for the Bi and Po region, triple humped for Ra and Ac region and to double humped for most of actinides systematically. However, further experimental studies are needed to clarify how the mass division mode changes as a function of the neutron number of the fissioning nuclide of the same Z .

ACKNOWLEDGMENTS

The authors wish to thank the staff and crew of the Japan Atomic Energy Research Institute (JAERI) Tandem Accelerator. We would like to thank Dr. N. Shinohara, Dr. S. Baba, K. Hata, S. I. Ichikawa, K. Tsukada, Dr. Y. Hatsukawa, and Dr. H. Ikezoe of JAERI, and I. Nishinaka, and Dr. K. Sueki of Tokyo Metropolitan University.

- [1] A. Turkevich and J. B. Niday, *Phys. Rev.* **84**, 52 (1951).
- [2] H. C. Britt, H. E. Wegner, and J. C. Gursky, *Phys. Rev.* **129**, 2239 (1963).
- [3] E. Konecny, H. J. Specht, and J. Weber, *Physics and Chemistry of Fission 1973* (IAEA, Vienna, 1974), Vol. II, p. 3.
- [4] J. Weber, H. C. Britt, A. Gavron, E. Konecny, and J. B. Wilhelmly, *Phys. Rev. C* **13**, 2413 (1976).

- [5] J. R. Nix and W. J. Swiatecki, *Nucl. Phys.* **71**, 1 (1965).
- [6] P. Möller and S. G. Nilsson, *Phys. Lett.* **31B**, 283 (1970).
- [7] V. M. Strutinsky, *Nucl. Phys.* **A95**, 420 (1967).
- [8] V. M. Strutinsky, *Nucl. Phys.* **A122**, 1 (1968).
- [9] Sven A. E. Johansson, *Nucl. Phys.* **22**, 529 (1961).
- [10] H. C. Pauli, T. Ledergerber, and M. Brack, *Phys. Lett.* **34B**, 264 (1971).
- [11] P. Möller, *Nucl. Phys.* **A192**, 529 (1972).

- [12] T. Ohtsuki, Y. Nagame, K. Tsukada, N. Shinohara, S. Baba, K. Hashimoto, I. Nishinaka, K. Sueki, Y. Hatsukawa, K. Hata, T. Sekine, I. Kanno, H. Ikezoe, and H. Nakahara, *Phys. Rev. C* **44**, 1405 (1991).
- [13] T. Ohtsuki, Y. Hamajima, K. Sueki, H. Nakahara, Y. Nagame, N. Shinohara, and H. Ikezoe, *Phys. Rev. C* **40**, 2144 (1989).
- [14] H. Kudo, H. Muramatsu, H. Nakahara, K. Miyano, and I. Kohno, *Phys. Rev. C* **25**, 3011 (1982).
- [15] Y. Hamajima, T. Ohtsuki, K. Sueki, and H. Nakahara (unpublished).
- [16] V. V. Pashkevich, *Nucl. Phys.* **A169**, 275 (1971).
- [17] U. Brosa, S. Grossman, and A. Müller, *Z. Naturf.* **41a**, 1341 (1986).
- [18] U. Brosa and S. Grossman, *Z. Phys. A* **310**, 177 (1983).
- [19] P. Möller, J. R. Nix, and W. J. Swiatecki, *Nucl. Phys.* **A469**, 1 (1987).
- [20] N. Bohr and J. A. Wheeler, *Phys. Rev.* **56**, 426 (1939).
- [21] F. Plasil and M. Blann, *Phys. Rev. C* **11**, 508 (1975).
- [22] B. B. Back, Ole Hansen, H. C. Britt, J. D. Garrett, and B. Leroux, *Physics and Chemistry of Fission 1973* (IAEA, Vienna, 1974), Vol. I, p. 3.
- [23] S. Bjørnholm and J. E. Lynn, *Rev. Mod. Phys.* **52**, 725 (1980).
- [24] A. Gavron, H. C. Britt, P. D. Goldstone, J. B. Wilhelmy, and S. E. Larsson, *Phys. Rev. Lett.* **38**, 1457 (1977).
- [25] C. F. Tsang and J. B. Wilhelmy, *Nucl. Phys.* **A184**, 417 (1972).
- [26] P. Möller and J. R. Nix, *Nucl. Phys.* **A229**, 269 (1974).
- [27] H. J. Specht, *Nucleonika* **20**, 717 (1975).
- [28] M. G. Itkis, V. N. Okolovich, A. Ya. Rusanov, and G. N. Smirenkin, *Yad. Fiz.* **41**, 849 (1985) [*Sov. J. Nucl. Phys.* **41**, 544 (1985)].
- [29] T. Ohtsuki, Ph.D. thesis, Tokyo Metropolitan University, 1990.